

Reducing the complexity of the Quantum Fourier Transform implementation

Byeongyong Park¹, Doyeol Ahn^{1,2,3*}

¹*Department of Electrical and Computer Engineering and Center for Quantum Information Processing, University of Seoul, 163 Seoulsiripdae-ro, Dongdaemun-gu, Seoul 02504, Republic of Korea.*

²*Physics Department, Charles E. Schmidt College of Science, Florida Atlantic University, 777 Glades Road, Boca Raton, FL 33431-0991, USA.*

³*First Quantum Inc., Majang-ro 195-14, Seongdong-gu, Seoul 94706, Republic of Korea.*

*Correspondence to: dahn@uos.ac.kr.

ABSTRACT

The quantum Fourier transform (QFT) is one of the most important quantum operations with wide range of application from integer factoring, quantum simulation, quantum Monte Carlo simulation for the option pricing to relatively new topic such as quantum algorithm for solving Navier-Stokes equation of the turbulent flow, to name a few. Major obstacle to the implementation of the QFT is the large number of elemental quantum gates needed to build the QFT. Of these resources needed for the implementation, the T-count and the T-depth are the major costs. So far, the existing best implementation of approximate quantum Fourier transform (AQFT) shows the T-count of $8n\log_2(n/\varepsilon)$ and the T-depth of $2n\log_2(n/\varepsilon)$ where n is the number of qubits and ε is the approximate error. Here, we propose the new approximation scheme of the QFT which halves both the T-count and the T-depth of the QFT of the best existing implementation. Our approach relies on the manipulation of R_z gates after the QFT decomposition and the application of the quantum Karnaugh map for systematic reduction. We report the detailed quantum circuits and the experimental verification of the proposed scheme using IonQ quantum computer though Amazon Braket cloud service. The quantum amplitude estimation algorithm (QAEA) which plays an essential role in solving nonlinear partial differential equations employs a QFT and an inverse QFT. This QAEA would be an exemplary quantum algorithm that can get the most benefit from our proposed scheme and can be applied

not only to financial engineering but also to solving Navier-Stokes equations for turbulent hyper sonic flow and numerical weather prediction that may have disruptive socio-economic impact, for which little attention is given.

INTRODUCTION

Quantum Fourier transform (QFT) is perhaps the most versatile component of quantum algorithms. Not only the QFT is the key ingredient in Shor algorithm¹, basic arithmetic operations²⁻⁵, solving linear systems of equations⁶, quantum phase estimation⁷, quantum counting⁸, quantum simulation⁹⁻¹², quantum sensing¹³, data fitting¹⁴, securities¹⁵⁻²⁰ but also the essential ingredient of more recent applications to financial engineering²² and solving Navier-Stokes fluid dynamics^{23,24}. In the latter, the QFT is used as an essential component of the quantum amplitude estimation algorithm²⁵⁻²⁷. Therefore, Improving the efficiency of the QFT implementation would be a pivotal task for many quantum algorithms.

Every quantum algorithm including the QFT are represented by the set of quantum circuits. A quantum circuit should be eventually decomposed into elementary gates for physical or logical execution. Efficient reduction of the complexity of large number of elemental quantum gates to build these quantum circuits with low error rate is a crucial step especially in the region of quantum computation with limited number of qubits. To prevent errors, quantum computers should be isolated from the environment because quantum information is very fragile from the decoherence caused by interactions. However, errors caused by interactions with the environment are not completely avoidable. There are some ways to reduce errors²⁸⁻³⁶. But these may be only temporary measures and eventually, the fault tolerant implementation of the elementary gates will be essential for large-scale quantum algorithms.

The Clifford gates can be used in a fault tolerant implementation of quantum circuits. These Clifford gates have the following properties: First, it was proved that a quantum circuit

consisting only of Clifford gates can be efficiently simulated by a classical computer³⁷ and Clifford gates can be implemented fault tolerantly at low cost³⁸. However, the Clifford gates are not universal, so the non-Clifford gates are also required. Among the non-Clifford gates, the $\pi/8$ gate (T) is generally selected for universality. A generator gate set of the Clifford group is the following: the Hadamard gate (H), the Phase gate (S), and the Controlled-NOT gate (CNOT). The set to which, the T gate is added to the set {H, S, CNOT}, is used as the standard elementary gate set. In the case of the T gate, it is impossible to implement fault tolerantly at low cost in contrast to the case normal Clifford gates³⁹. To generate the T gate in a fault-tolerant way, magic state distillation may be required⁴⁰. And this is much more expensive than the implementation of Clifford gates fault-tolerantly. So, for the fault tolerant quantum computing using Clifford + T gate set, the T-count and the T-depth are considered as the major costs of the implementation. There have been many studies to reduce T-count and T-depth for various circuits⁴¹⁻⁵⁴.

Quantum circuits are expressed as intermediate gates like the swap gates, or the controlled phase gates before being decomposed into elementary gates. The textbook n qubit QFT circuit consists of $n(n-1)/2$ controlled phase gates, $[n/2]$ swap gates, and n Hadamard gates⁵⁵. A swap gate can be synthesized using 3 CNOT gates. There are many proposed methods in the previous studies to implement controlled phase gates^{43,56,57}. In general, synthesis of a controlled phase gate requires R_n gates (equivalent to the R_z gate up to global phase) in addition to elementary gates. Complete decomposition of a general R_z gate in the standard elementary gate set is not possible. Therefore, for the R_z gate implementation, the gate synthesis is used with error bound for the algorithm^{48,54}, or addition with some special quantum state is used to execute the layer of R_z gates^{51,52,58}. In the case of gate synthesis, if measurement and an ancilla qubit are used, the T-count required for an R_z gate synthesis is known to be $1.15\log_2(1/\varepsilon)$ with the precision ε by using repeat-until-success (RUS) circuits⁵⁴. To use addition instead of R_z gates

implementation, it is necessary to create a serial R_z gate layer to make a phase gradient transformation. This is not a generally available method. But for the QFT, it is possible to create such an R_z layer⁵².

$$\text{Controlled phase} = \begin{pmatrix} 1 & 0 & 0 & 0 \\ 0 & 1 & 0 & 0 \\ 0 & 0 & 1 & 0 \\ 0 & 0 & 0 & e^{i\pi/2^{n-1}} \end{pmatrix},$$

$$R_n = \begin{pmatrix} 1 & 0 \\ 0 & e^{i\pi/2^{n-1}} \end{pmatrix}, \quad R_z(\theta) = e^{-i\theta/2} \begin{pmatrix} 1 & 0 \\ 0 & e^{i\theta} \end{pmatrix} \quad (1)$$

The approximate Quantum Fourier transform (AQFT) has been studied for implementation of the QFT in a fault tolerant manner or in the presence of decoherence^{52,59-62}. The AQFT is an approximate version of QFT by excluding controlled phase gates with rotation angles less than a certain value from the QFT. In this approximation, the standard choice for the n qubit AQFT is to keep only $O(n\log n)$ controlled phase gates. The reason why AQFT is studied widely is that the exact implementation of the general QFT is not the option as of now when the circuit is executed using Clifford + T gate set. Because there is no way to implement general controlled phase gates or R_z gate using known gate synthesis method. And if addition is used to implement the R_z gate layer, the state like $|\psi\rangle = \frac{1}{\sqrt{2^{b+1}}} \sum_{k=0}^{2^{b+1}-1} e^{2\pi i k / 2^{b+1}} |k\rangle$ must be prepared. To prepare the state, the synthesis of R_z gates is required even once. Therefore, with Clifford + T gate set, there is no choice but to implement approximation of the QFT with some precision ε . When implementing the QFT with error of $O(\varepsilon)$ using AQFT, only controlled phase gates with a rotation angle greater than $\sim [\pi/2^{\log_2(\frac{n}{\varepsilon})}]$ remain in the n qubit AQFT. The smallest T-count known so far for the n qubit AQFT implementation is $\sim 8n\log_2(n/\varepsilon)$, and T-depth is $\sim 2n\log_2(n/\varepsilon)$.⁵²

Recently, one of the authors proposed an efficient quantum circuit optimization method based on the quantum Karnaugh map.⁶³ In this paper, we introduce a new implementation of the QFT using quantum Karnaugh map and other methods, which shows $\sim 50\%$ reduction of the best

known⁵² T-count and T-depth results. To reduce the T-count, First, we decompose the full QFT circuit into the proper R_z and CNOT gates. Second, some of the R_z gates are replaced with S gate or discarded for approximation. Using this method, we get T-count of $\sim 4n\log_2(n/\varepsilon)$ with error of $O(\varepsilon)$. It has T-depth of $\sim 2n\log_2(n/E)$. To reduce T-depth without significant penalty of T-count, we modify Peter Selinger's method⁵³, and apply the scheme that we propose to reduce T-count. As a result, we implement the QFT circuit with error $O(\varepsilon)$ at a cost of $\sim 4n\log_2(n/\varepsilon)$ T-count and $\sim n\log_2(n/\varepsilon)$ T-depth which is the half of the best known result⁵². We also show some preliminary experimental verification results using Amazon Braket cloud quantum computation service.

RESULT AND DISCUSSION

Scheme 1

In scheme 1, we reduce the T-count of the QFT circuit. Details of the intermediate circuits in the process can be found in the supplementary information. First, we decompose sub-circuits of the textbook QFT circuit⁵⁵ [Fig. 1a]. The sub-circuits are composed of gates from a beginning Hadamard gate to the next Hadamard gate. We then decompose the controlled phase gates to CNOT gates and R_z gates using the Fig. 5 of the ref. ⁵⁶[Fig. 2a]. In this process, a reusable ancilla qubit in the state $|0\rangle$ is used. We then cancel CNOT gates between the adjacent decomposed controlled phase gates and unite the R_z gates acting on the ancilla qubit. Next we move the R_z gates at the top of the decomposed controlled phase gate to the left of the sub-circuit. Here, moving a gate to the left in the circuit means repositioning the gate so that it is executed earlier in the circuit. By doing so, it is possible to obtain one R_z gate layer composed of $R_z(\pi/4)$, $R_z(\pi/8)$, ... $R_z(\pi/2^k)$ per one sub-circuit. The all R_z gate layers from the sub-circuits made by the process above can be moved to the left end of the QFT circuit and combined into one R_z gate layer at the very beginning of the circuit. Here, we introduce the circuit identity 1

in Fig. 2b. It can be proved by showing that the quantum Karnaugh maps⁶³ of the two circuits of Fig. 2b are the same. A brief description of the quantum Karnaugh map can be found in the method section. By applying circuit identity 1 in Fig. 2b, the remaining gates in each sub-circuit can be reorganized into a circuit having one R_z gate layer. Next, using the circuit identity 2 in Fig. 2c⁵³, we can move the R_z gate from the ancilla qubit to the right side of the qubit which includes the H gate of the sub-circuit. In this process, the ancilla qubit is eliminated. The moved R_z gates of each sub-circuit can be moved more to the right end of the QFT circuit and these R_z gates constitute one R_z gate layer at the end of the total circuit. This R_z gate layer has the same components as the R_z gate layer we constitute at the beginning of the total circuit, but the order is reversed. As a result, we reconstruct the QFT circuit into the circuit in Fig. 1b, and it has only $(n + 1)$ R_z gate layers.

So far, it is a perfect QFT implementation without any approximation. Now we proceed with approximation in a different way from the AQFT. The conventional AQFT discards some controlled phase gates, but here we decompose the QFT circuit into R_z and CNOT gates, and then discard some R_z gates. First, the R_z gates in the first and last R_z gate layers are replaced with the form of S gate ($= R_z(\pi/2) + R_z(-\pi/2^k)$) gate. And All the R_z gates with a rotation angle less than $\pi/2^b$ are discarded. Then, up to $(b - 1)$ R_z gates except S gates remain in each R_z gate layer. [Fig. 1c]

The R_z gate layer consisting of $R_z(-\pi)$, $R_z(-\pi/2)$, $R_z(-\pi/4)$, ..., $R_z(-\pi/2^t)$ can be implemented using modulo 2^{t+1} addition if the state $|\psi\rangle = \frac{1}{\sqrt{2^{t+1}}} \sum_{k=0}^{2^{t+1}-1} e^{2\pi i k / 2^{t+1}} |k\rangle$ is prepared⁵⁸.

And the state $|\psi\rangle$ is reusable. This is possible because there is periodicity both in the exponential function and in the modulo addition. To implement R_z gate layers in the circuit of Fig. 1c using addition, since there are no $R_z(-\pi)$ and $R_z(-\pi/2)$ gates for all R_z gate layers in Fig. 1c, S and Z gates are added in each R_z gate layer. And to cancel the effect of these gates, S^+ and Z^+ gates are also added next to each S and Z gate. And then, all the $(n + 1)$ R_z gate layers

in our scheme are in the form that can be executed using addition. Therefore, we implement up to $(b + 1)$ qubit addition n times for the circuit implementation. This is because the n th R_z gate layer does not require addition since it consists only of T gate. In the case of R_z gate layers in which the absolute value of smallest angle of R_z gates is $\pi/2^k$ and k is smaller than b , $(k + 1)$ qubit addition is applied. In the process, the required state $|\psi_{k+1}\rangle = \frac{1}{\sqrt{2^{k+1}}} \sum_{j=0}^{2^{k+1}-1} e^{2\pi i j / 2^{k+1}} |j\rangle$ does not need to be prepared separately, because the corresponding part of $|\psi\rangle$ can be used.

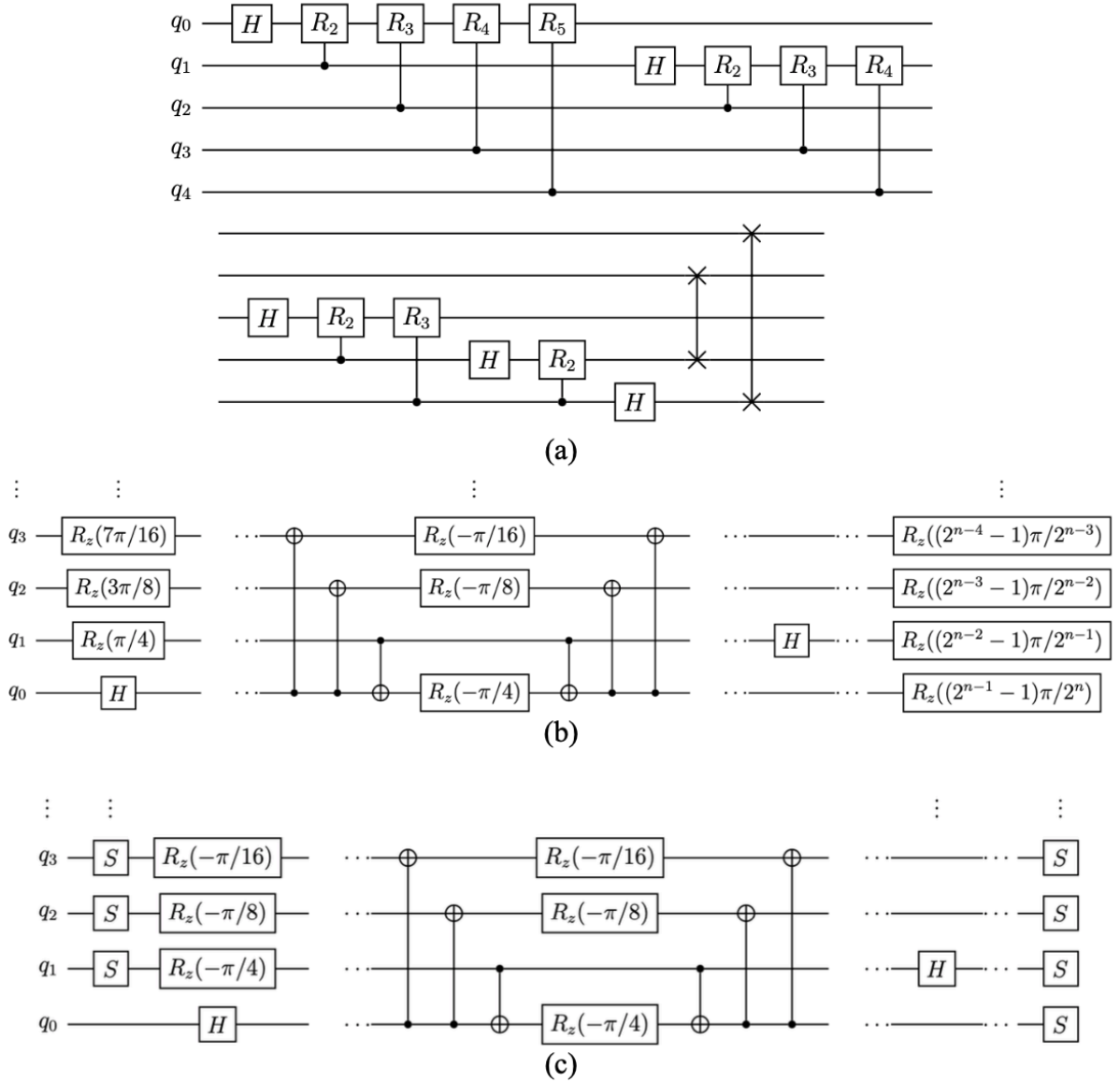
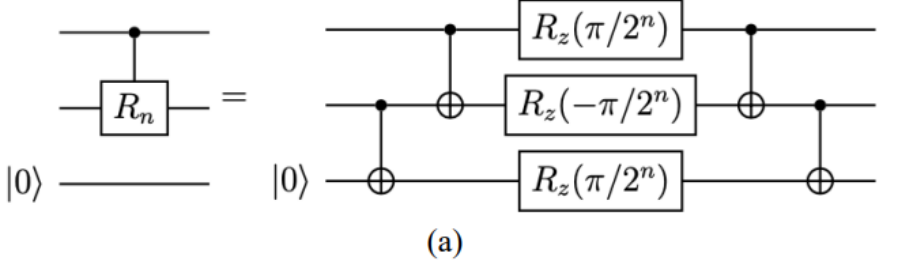
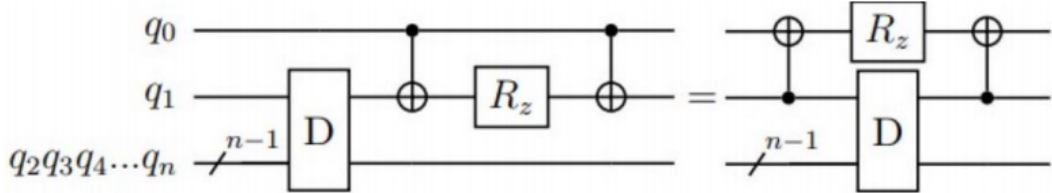


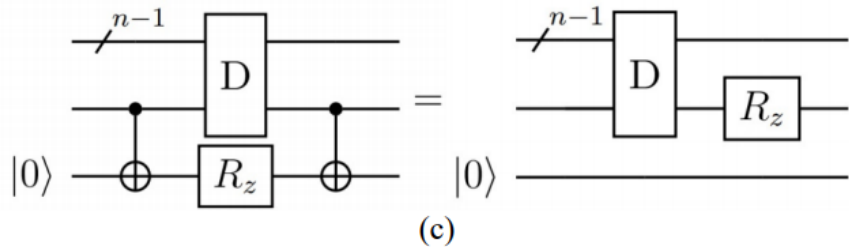
Fig. 1 Circuits in scheme 1. **a** Textbook⁵⁵ 5 qubit QFT circuit; **b** n qubit QFT circuit with $(n+1)$ R_z gate layer without approximation; **c** n qubit QFT circuit with approximation.



(a)



(b)



(c)

Fig.2 Circuit identities. **a** Controlled phase gate decomposition in ref⁵⁶; **b** Circuit identity 1 and its quantum Karnaugh map⁶³. The matrix representation of D using computational basis is a diagonal matrix, R_z is an z rotation gate with arbitrary rotation angle θ , and q_0, q_1, \dots, q_n are qubits from the top of the circuits; **c** Circuit identity 2. It is from the ref⁵³.

Implementation on the actual quantum hardware

Quantum computers in the noisy intermediate-scale quantum (NISQ)²¹ era should be built in a way that reduces decoherence. In the process of scheme 1, even if using addition and approximation are excluded, we note that the circuit in Fig. 1b is suitable for the implementation on a NISQ machine because of its reduced circuit depth. So we implemented

quantum phase estimation(QPE) using the QFT circuit in Fig. 1b to see if we get the proper results when we apply our decomposition method to quantum algorithm. QPE is an algorithm to find the eigenvalue $e^{2\pi i\varphi}$ of a unitary matrix U using the corresponding eigenvector $|u\rangle$ ⁵⁵.

We define the matrix U and the eigenvector $|u\rangle$ as follows.

$$U = \begin{pmatrix} 1 & 0 \\ 0 & e^{2\pi i\varphi} \end{pmatrix}, \quad |u\rangle = \begin{pmatrix} 0 \\ 1 \end{pmatrix} \quad (2)$$

QPE is implemented using controlled U gates and an inverse quantum Fourier transform. We executed the inverse quantum Fourier transform and controlled U gates using the same method with the circuit decomposition of Fig. 1b and implemented on the IonQ device using Amazon Braket. To clarify that it is an n qubit QPE, we fixed the last qubit as $|1\rangle$ of the angles φ , and remaining qubits were set at random. We chose φ 0.0111 for 4 qubit, 0.01001 for 5 qubit, 0.100101 for 6 qubit, 0.1110101 for 7 qubit, 0.01001111 for 8 qubit, and 0.110001011 for 9 qubit. As a result, the correct answer was obtained with a majority value in 4-9 qubit QPE.

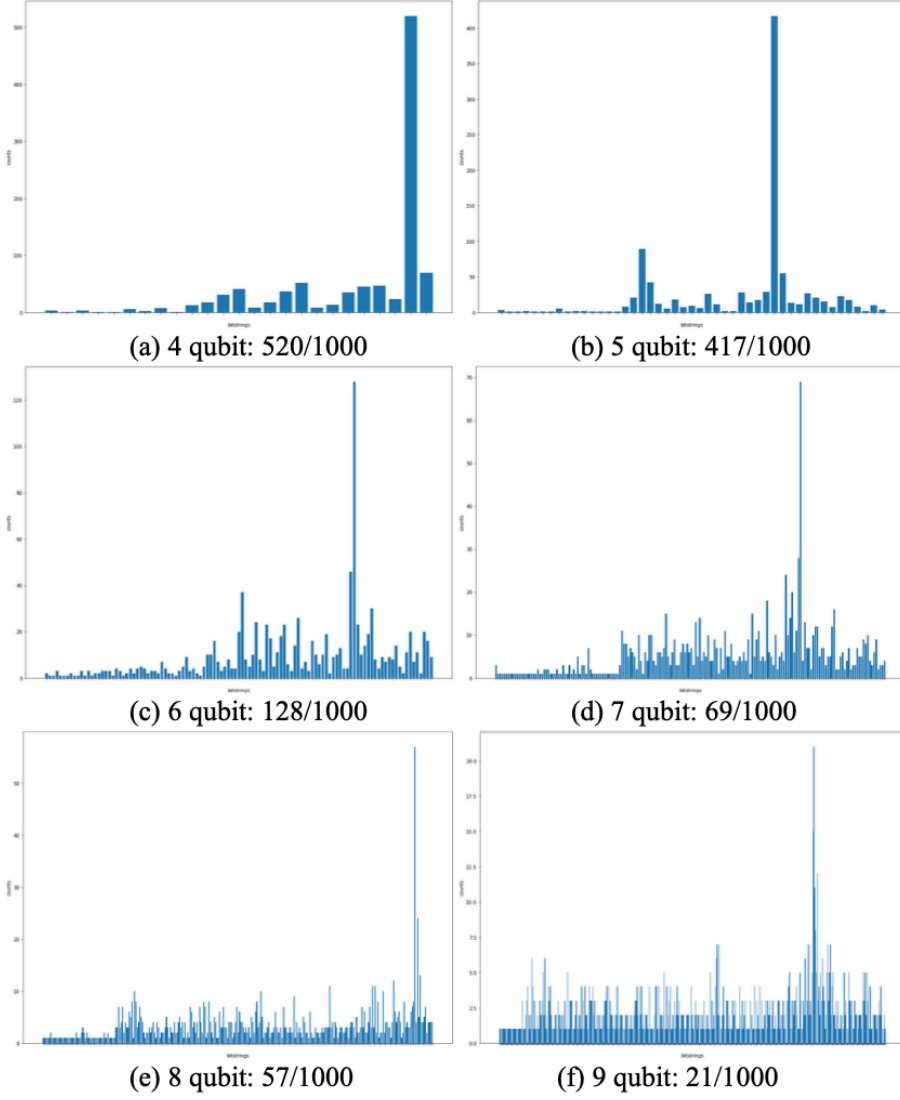


Fig. 3 QPE implementation on the quantum hardware(IonQ). $\varphi = 0.0111$ for 4-qubit, 0.01001 for 5-qubit, 0.100101 for 6-qubit, 0.1110101 for 7-qubit, 0.01001111 for 8-qubit, and 0.110001011 for 9-qubit. (a/b) means (correct answer/trial). Only when the eigenvector used was remained $|1\rangle$, it is counted as the correct answer.

Error and Result of Scheme 1

The error between U and V gate or precision of implementation of U instead of V is defined as the spectral norm of $(U - V)$ and the accumulative error between $U_1 U_2 \dots U_m$ and $V_1 V_2 \dots V_m$ is at most the sum of the error between U_i and V_i ⁵⁵. If one $R_z(-\pi/2^k)$ gate is discarded, the error is $\|(1 - e^{i\pi/2^k})\|$, and it is smaller than $\pi/2^k$. So, the maximum error of the first R_z gate layer in

Fig. 1c is at most $\sum_{k=b+1}^n (\pi/2^k) \leq \pi/2^b$. Since the error of the first R_z gate layer is the greatest among the errors of the R_z gate layers, the upper bound of the error because of the discarded R_z gates is $\pi(n-b+2)/2^b$. If we choose b as $\log_2(n/\varepsilon)$, The error is lower than $\pi(n-b+2)\varepsilon/n < \pi\varepsilon = O(\varepsilon)$ (we assume $b \geq 2$).

The total error is not dependent on only the error because of discarded R_z gates but also the error because of gate synthesis. Gate synthesis is necessary for the preparation of state $|\psi\rangle$ which is used for addition. Before implementing $(b+1)$ qubit addition, The state $|\psi\rangle = \frac{1}{\sqrt{2^{b+1}}} \sum_{k=0}^{2^{b+1}-1} e^{2\pi i k / 2^{b+1}} |k\rangle$ is needed, and the state $|\psi\rangle$ can be obtained by respectively executing a Hadamard gate and the $R_z(\pi/2^k)$ gate on the k th qubit in the $(b+1)$ qubits which is initially in the $|0\rangle$ state. Therefore, $(b+1)$ R_z gates should be synthesized. Among them, Z, S, and T gates do not need to be synthesized, so a total of $(b-2)$ R_z gates need to be synthesized. If the repeat-until-success circuit (RUS) with an ancilla qubit and measurement is used, the expected smallest T-count known so far to synthesize an R_z gate using Clifford + T gates with error ε is $\sim 1.15\log_2(1/\varepsilon)$. If we choose the precision of gate synthesis as ε/b , The error because of gate synthesis is lower than $\varepsilon(b-2)/b < \varepsilon$. Then, the total error ε is lower than $(\pi+1)\varepsilon$. So, the error between QFT and our approximation scheme is $O(\varepsilon)$.

The required number of the T gates to implement scheme 1 is divided into two parts. The first one is the T gates required for addition. For m qubit addition, the smallest known T-count so far is $4(m-1)$.⁵¹ Since we need roughly $(b+1)$ qubit addition n times, The T-count for addition is $\sim 4nb = 4n\log(n/\varepsilon)$. The other one is the T gates required for gate synthesis. Because there are $(b-2)$ R_z gates which need gate synthesis, T-count required for gate synthesis is $\sim (b-2)(1.15\log_2(b/\varepsilon)) = 1.15(\log_2(n/\varepsilon)-2)(\log_2(\log_2(n/\varepsilon)/\varepsilon))$. So the total T-count is $\sim 4n\log_2(n/\varepsilon) + 1.15(\log_2(n/\varepsilon)-2)(\log_2(\log_2(n/\varepsilon)/\varepsilon)) \sim 4n\log_2(n/\varepsilon)$ with error of $O(\varepsilon)$. And in this case, The T-depth is $\sim 2nb + 1.15\log_2(b/\varepsilon) \sim 2n\log_2(n/\varepsilon)$. The $2nb$ term is from the adders. Because the T-depth required for a $(b+1)$ qubit adder is $2b$ ⁵¹ and n additions are applied. $1.15\log_2(b/\varepsilon)$ term

is from the gate synthesis. The reason why $(b - 2)$ doesn't have to be multiplied is that each gate synthesis can be implemented in parallel.

Scheme 2

In scheme 2, when comparing the leading order term, we reduce T-depth by half and maintain T-count compared to scheme 1 in the same order of error. The process of scheme 2 is as follows. First, we move the even-numbered H gate to the left in the textbook QFT circuit in Fig. 1a as far as possible like Fig. 4a. Here, the number of modified sub-circuits between Hadamard gates in the n qubit QFT is $(n - 1)$. Among these $(n - 1)$ sub-circuits, $[n/2]$ are controlled S gate. And the controlled S gate can be decomposed into a circuit having T-depth 1 and T-count 3 using the circuit decomposition in Fig. 2a. The remaining $[(n-1)/2]$ sub-circuits can be decomposed in the same manner as scheme 1. The process results in circuits with two R_z gate layers for each $[(n - 1)/2]$ sub-circuit. Like scheme 1, the newly created two R_z layers are appended to the left and right ends of the QFT circuit. Next, we approximate the QFT as scheme 1 by discarding R_z gates with rotation angle below $\pi/2^b$ [Fig. 4b] Here, we introduce theorem 1 to reduce the R_z gate depth. This is a slight variation of Theorem 4.1 of ref. ⁵³.

Theorem 1. A circuit consisting of only R_z and CNOT gates can be reorganized by a circuit that has only one R_z gate layer.

(Proof) The proof of theorem 1 follows the proof of Theorem 4.1 of ref. ⁵³ exactly. In the proof, we use the circuit representation and its matrix representation using computational basis interchangeably. That is, we write the matrix representation of circuit C as C when there is no room for confusion. And $\text{CNOT}(a;b)$ refers to a CNOT gate in which the control qubit is a and the target qubit is b. Theorem 1 is proved by showing that its sufficient condition is true. The sufficient condition is that for any circuit A consisting only of R_z gates and CNOT gates, there are always circuits D and R_0 where $A = R_0D$. Here, D is a diagonal matrix, and the number of

R_z gate layers included in D is 0 or 1. R_0 consists of only CNOT gates. This proposition is proved by using mathematical induction. If circuit A doesn't include any gates, then both D and R_0 are I . Suppose that for an arbitrary circuit A' which consists of n R_z or CNOT gates, there are R_0' and D' that satisfy the conditions. When $(n + 1)$ th gate is added to circuit A' , if the added gate is $CNOT(a;b)$, then $A = A'CNOT(a;b) = R_0'D'CNOT(a;b) = R_0'CNOT(a;b)CNOT(a;b)D'CNOT(a;b)$. Here, R_0 is $R_0'CNOT(a;b)$ and D is $CNOT(a;b)D'CNOT(a;b)$. If the added gate is R_z gate, then $A = A'R_z = R_0'D'R_z$. Here, R_0 is R_0' , and $D'R_z$ can be reconstituted into a new D by using the circuit identity 2 in Fig. 2c. In this process, an ancilla qubit which is in the state $|0\rangle$ and two CNOT gates are required as costs.

In the circuit of Fig. 4b, It can be seen that $[(n - 1)/2]$ sub-circuits with two R_z layers consist of only R_z gates and CNOT gates. Therefore, we can apply theorem 1 to the sub-circuits [Fig. 4c] to make circuits with R_z layer one. With $[(n - 1)/2]$ sub-circuits with one R_z gate layer, we can reduce the leading order term of T-depth of the QFT by half by allowing the two $(b + 1)$ qubit additions to be implemented in parallel.

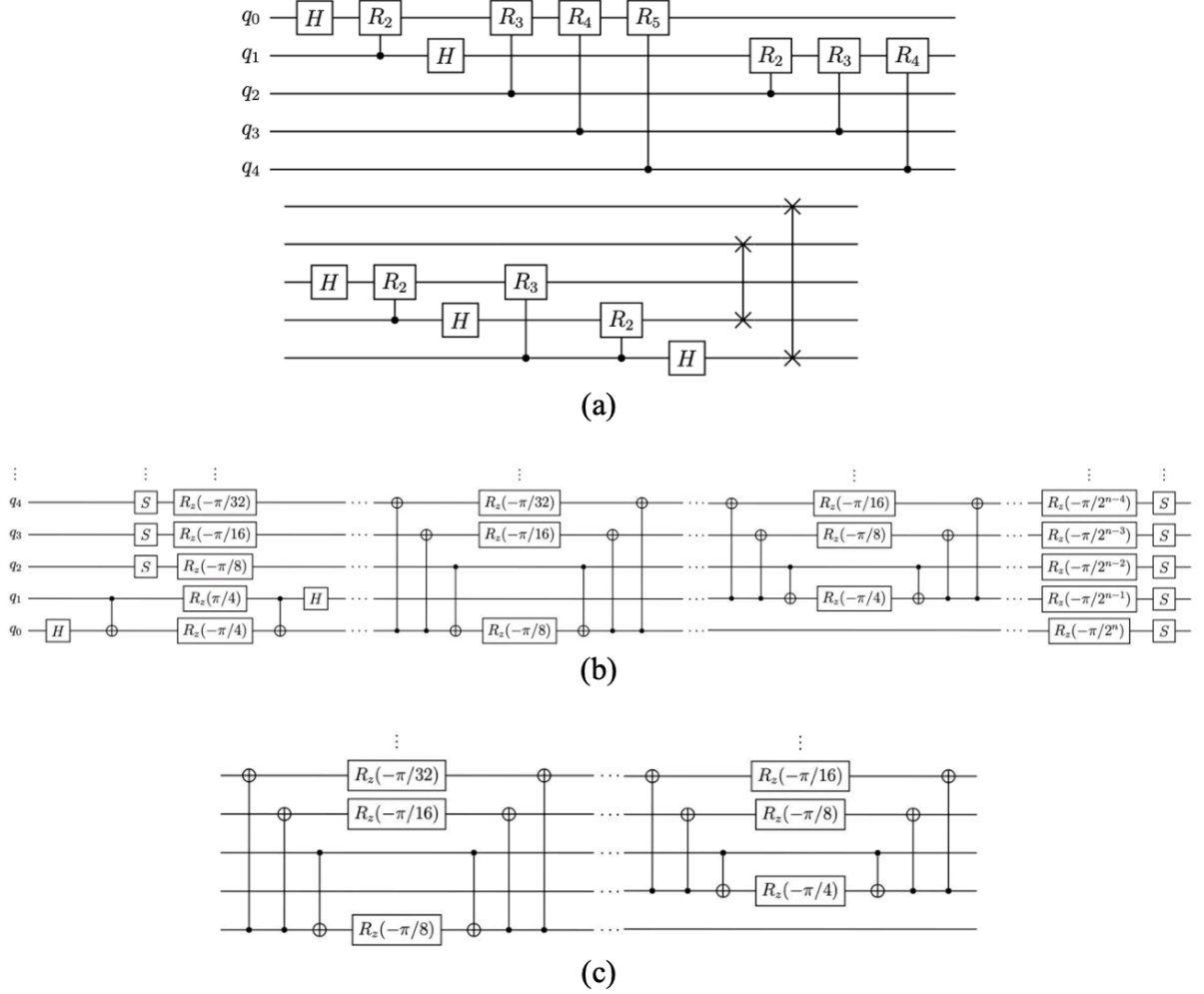


Fig. 4 Circuits in scheme 2. a 5 qubit QFT circuit with moved Hadamard gates; **b** QFT circuit before theorem 1 is applied; **c** The form of sub-circuits to which theorem 1 is applied.

Error and Result of Scheme 2

Compared to scheme 1, The only thing that can change the order of total error in Scheme 2 is that one more $|\psi\rangle$ needs to be prepared. This requires $(b - 2)$ additional R_z gate synthesis. If we choose the precision of gate synthesis as $\varepsilon/2b$, the error because of gate synthesis is lower than ε . Then the total error is the same as $O(\varepsilon)$.

From the perspective of T-count, $\sim 2.3(b - 2)\log_2(2b/\varepsilon)$ T gates are required to prepare two $|\psi\rangle$. This requires more $\sim 1.15(b - 2)(\log(b/\varepsilon) + 2)$ T gates than scheme 1. There are additional $\sim n$ T gates required more than scheme 1 in the circuit before applying addition. About half of

them are R_z gates at the target qubit of controlled S gate decomposition and the rest are appended ones to R_z layers which don't have $R_z(-\pi/4)$ to apply addition. Therefore, The number of T gates required more than scheme 1 is $\sim n + 1.15(b - 2)(\log(b/\varepsilon) + 2)$, and this does not change the leading order term $4n\log_2(n/\varepsilon)$. T-depth of the QFT implemented scheme 2 is $2b[(n - 1)/2] + [n/2] + 1.15\log(2b/\varepsilon) \sim n\log_2(n/\varepsilon)$. $2b[(n - 1)/2]$ term is from the adder depth, $[n/2]$ term is due to the T gates on the target qubit in the controlled S gate decompositions which do not use adder, and $1.15\log_2(2b/\varepsilon)$ term is from the parallel gate synthesis. If $n < 2(b - 2)$, for the parallel gate synthesis, additional ancilla qubits are needed. Even if the parallel gate synthesis is not used, the leading order term of the T-depth of scheme 2 does not change. In short, in scheme 2, we reduce the T-depth by about half with the same order of error and the same leading order term of T-count compared to scheme 1. And the cost of reducing T-depth is additional $\sim n$ T gates, $\sim 2n\log(n/\varepsilon)$ CNOT gates, and $\sim 2b$ qubits.

Conclusion

In this paper, we introduced a new approximation of QFT with the error of $O(\varepsilon)$. This approximation has the T-count of $\sim 4n\log_2(n/\varepsilon)$ and the T-depth of $\sim n\log_2(n/\varepsilon)$ with the error of $O(\varepsilon)$. To the best of our knowledge, $\sim 8n\log_2(n/\varepsilon)$ T-count with $\sim 2n\log_2(n/\varepsilon)$ T-depth is the best known result for least T-count and T-depth implementation of QFT using AQFT with the error of $O(\varepsilon)^{52}$. So, the T-count of scheme 1 is approximately half compared to the conventional AQFT with the same T-depth roughly. And we reduced T-depth from $\sim 2n\log_2(n/\varepsilon)$ to $\sim n\log_2(n/\varepsilon)$ without changing the leading order of T-count using the parallelly applied adders in scheme 2. Therefore, our results show the 50% reduction of the best known T-count and T-depth complexity.

Comparison with AQFT

If the circuit decomposition method used in scheme 1 is applied to conventional AQFT with the error of $O(\varepsilon)$, the number of T gates required is $\sim 6.3\log_2(n/\varepsilon)$ with $\sim 2n\log_2(n/\varepsilon)$ T-depth. Because $\sim (2n-b)$ R_z gates need gate synthesis, so $\sim 1.15\log_2(2n/\varepsilon)$ T gates are required per one R_z gate approximation to get the error of $O(\varepsilon)$, and consequently this affects the leading order term of T-count. Applying our scheme to the conventional AQFT is more efficient than the previously known implementation method of AQFT⁵², but it costs more compared to scheme 1 and 2 we proposed.

Limitation and future work

First, our study does not suggest the theoretical lower bound of the T-count or T-depth of QFT. Therefore, future research topics may include presenting the lower bound of T-count or T-depth of QFT with the error of $O(\varepsilon)$ and finding an implementation method close to the bound. In addition, in the case of scheme 2, costs except the leading order term of the T-count were not considered. Scheme 2 required additional $O(n)$ of T gates, $O(b)$ of qubits, and $O(n\log(n/\varepsilon))$ of CNOT gates compared to scheme 1. This is a considerable cost. So future studies may include reducing T-depth without significantly changing T-count, the number of qubits, and CNOT gates.

The QFT is widely used in various quantum algorithms including quantum security, option pricing, quantum Monte Carlo simulation and even solving the Navier-Stokes equation of the fluid dynamics. For example, the quantum amplitude estimation algorithm (QAEA) uses a QFT and an inverse QFT in its implementation. With our approach, one may expect a 50% reduction of the QAEA implementation for the first register which in turn would provide substantial speed-ups of the quantum algorithm execution. Therefore our implementation would open up the practical applications of quantum computers.

METHODS

Quantum Karnaugh map⁶³

Quantum Karnaugh map (QKM), like classical Karnaugh map, is to write the possible cases in the table. Since quantum information is continuous, it may be considered difficult to write in a table. However, because quantum mechanics is linear, it is sufficient to consider only the case for computational basis. In the table, each cell is filled with the matrix or number acting on each computational basis. If the two quantum Karnaugh maps of two circuits are the same, then the two circuits are circuits that perform the same operation.

DATA AVAILABILITY

Intermediate circuits in the schemes can be found in the supplementary information. The other data of this study are available from the authors upon reasonable request.

CODE AVAILABILITY

The code used to run the QPE using Amazon Braket can be found in the supplementary information.

REFERENCES

1. Shor, P. W. Polynomial-time algorithms for prime factorization and discrete logarithms on a quantum computer. *SIAM review* 41, 303–332 (1999).
2. Draper, T. G. Addition on a quantum computer. *arXiv preprint quant-ph/0008033* (2000).
3. Ruiz-Perez, L. & Garcia-Escartin, J. C. Quantum arithmetic with the quantum Fourier transform. *Quantum Information Processing* 16, 1–14 (2017).
4. Şahin, E. Quantum arithmetic operations based on quantum Fourier transform on signed integers. *International Journal of Quantum Information* 18, 2050035 (2020).

5. Pachau, J. L., Roy, A. & Saha, A. K. Integer numeric multiplication using quantum Fourier transform. *Quantum Studies: Mathematics and Foundations* 1–10 (2021).
6. Harrow, A. W., Hassidim, A. & Lloyd, S. Quantum algorithm for linear systems of equations. *Physical review letters* 103, 150502 (2009).
7. Kitaev, A. Y. Quantum measurements and the Abelian stabilizer problem. *arXiv preprint quant-ph/9511026* (1995).
8. Brassard, G., Høyer, P. & Tapp, A. Quantum counting. in *International Colloquium on Automata, Languages, and Programming* 820–831 (Springer, 1998).
9. Aspuru-Guzik, A., Dutoi, A. D., Love, P. J. & Head-Gordon, M. Simulated quantum computation of molecular energies. *Science* 309, 1704–1707 (2005).
10. Lidar, D. A. & Wang, H. Calculating the thermal rate constant with exponential speedup on a quantum computer. *Physical Review E* 59, 2429 (1999).
11. Benenti, G. & Strini, G. Quantum simulation of the single-particle Schrödinger equation. *arXiv preprint arXiv:0709.1704* (2007).
12. Kassal, I., Whitfield, J. D., Perdomo-Ortiz, A., Yung, M.-H. & Aspuru-Guzik, A. Simulating chemistry using quantum computers. *Annual review of physical chemistry* 62, 185–207 (2011).
13. Vorobyov, V. et al. Quantum Fourier transform for nanoscale quantum sensing. *npj Quantum Information* 7, 1–8 (2021).
14. Wiebe, N., Braun, D. & Lloyd, S. Quantum algorithm for data fitting. *Physical review letters* 109, 050505 (2012).
15. Zhang, W.-W., Gao, F., Liu, B., Wen, Q.-Y. & Chen, H. A watermark strategy for quantum images based on quantum Fourier transform. *Quantum information processing* 12, 793–803 (2013).
16. Yang, Y.-G., Jia, X., Sun, S.-J. & Pan, Q.-X. Quantum cryptographic algorithm for color

images using quantum Fourier transform and double random-phase encoding. *Information Sciences* 277, 445–457 (2014).

17. Mashhadi, S. General secret sharing based on quantum Fourier transform. *Quantum Information Processing* 18, 1–15 (2019).

18. Yang, W., Huang, L., Shi, R. & He, L. Secret sharing based on quantum Fourier transform. *Quantum information processing* 12, 2465–2474 (2013).

19. Yang, Y.-G., Xia, J., Jia, X. & Zhang, H. Novel image encryption/decryption based on quantum Fourier transform and double phase encoding. *Quantum information processing* 12, 3477–3493 (2013).

20. Zhang, C., Razavi, M., Sun, Z. & Situ, H. Improvements on “Secure multi-party quantum summation based on quantum Fourier transform”. *Quantum Information Processing* 18, 1–12 (2019).

21. Preskill, J. Quantum computing in the NISQ era and beyond. *Quantum* 2, 79 (2018).

22. Stamatopoulos, N., Egger, D. J., Sun, Y., Zoufal, C., Iten, R., Shen, N. & Woerner, S. Option pricing using quantum computers. arXiv:1905.02666 (2020).

23. Gaitan., F. Finding flows of a Navier-Stokes fluid through quantum computing. *npj Quantum Inf.* 6, 61 (2020).

24. Gaitan, F. Finding Solutions of the Navier-Stokes equations through quantum computing—recent progress, a generalization and next steps forward. *Adv. Quantum Technol.* 4, 2100055 (2021)

25. Brassard, G., Hoyer, P., Mocca, M. & Tapp, A. Quantum amplitude amplification and estimation. *Contemporary Mathematics* 305 (2002), 10.1090/conm/305/05214.

26. Grover, L. K. Quantum mechanics helps in searching for a needle in a haystack. *Phys. Rev. Lett.* 79, 325-328 (1997).

27. Novak, E. Quantum complexity of integration. *J. Complexity* 17, 2-16 (2001).

28. Saki, A. A., Alam, M. & Ghosh, S. Study of decoherence in quantum computers: A circuit-design perspective. arXiv preprint arXiv:1904.04323 (2019).

29. Nash, B., Gheorghiu, V. & Mosca, M. Quantum circuit optimizations for NISQ architectures. *Quantum Science and Technology* 5, 025010 (2020).

30. Wilson, E., Singh, S. & Mueller, F. Just-in-time quantum circuit transpilation reduces noise. in 2020 IEEE International Conference on Quantum Computing and Engineering (QCE) 345–355 (IEEE, 2020).

31. Strikis, A., Qin, D., Chen, Y., Benjamin, S. C. & Li, Y. Learning-based quantum error mitigation. *PRX Quantum* 2, 040330 (2021).

32. Kim, C., Park, K. D. & Rhee, J.-K. Quantum error mitigation with artificial neural network. *IEEE Access* 8, 188853–188860 (2020).

33. Endo, S., Benjamin, S. C. & Li, Y. Practical quantum error mitigation for near-future applications. *Physical Review X* 8, 031027 (2018).

34. Temme, K., Bravyi, S. & Gambetta, J. M. Error mitigation for short-depth quantum circuits. *Physical review letters* 119, 180509 (2017).

35. Gheorghiu, V., Li, S. M., Mosca, M. & Mukhopadhyay, P. Reducing the CNOT count for Clifford+ T circuits on NISQ architectures. arXiv preprint arXiv:2011.12191 (2020).

36. McKay, D. C., Wood, C. J., Sheldon, S., Chow, J. M. & Gambetta, J. M. Efficient Z gates for quantum computing. *Physical Review A* 96, 022330 (2017).

37. Gottesman, D. The Heisenberg representation of quantum computers. arXiv preprint quant-ph/9807006 (1998).

38. Gottesman, D. Theory of fault-tolerant quantum computation. *Physical Review A* 57, 127 (1998).

39. Eastin, B. & Knill, E. Restrictions on transversal encoded quantum gate sets. *Physical review letters* 102, 110502 (2009).

40. Bravyi, S. & Kitaev, A. Universal quantum computation with ideal Clifford gates and noisy ancillas. *Physical Review A* 71, 022316 (2005).

41. Biswal, L., Das, R., Bandyopadhyay, C., Chattopadhyay, A. & Rahaman, H. A template-based technique for efficient clifford+ t-based quantum circuit implementation. *Microelectronics Journal* 81, 58–68 (2018).

42. Thapliyal, H., Munoz-Coreas, E., Varun, T. S. S. & Humble, T. S. Quantum circuit designs of integer division optimizing T-count and T-depth. *IEEE Transactions on Emerging Topics in Computing* 9, 1045–1056 (2019).

43. Amy, M., Maslov, D., Mosca, M. & Roetteler, M. A meet-in-the-middle algorithm for fast synthesis of depth-optimal quantum circuits. *IEEE Transactions on Computer-Aided Design of Integrated Circuits and Systems* 32, 818–830 (2013).

44. Maslov, D. Advantages of using relative-phase Toffoli gates with an application to multiple control Toffoli optimization. *Physical Review A* 93, 022311 (2016).

45. Gheorghiu, V., Mosca, M. & Mukhopadhyay, P. T-count and T-depth of any multi-qubit unitary. *arXiv preprint arXiv:2110.10292* (2021).

46. Thapliyal, H., Munoz-Coreas, E., Varun, T. S. S. & Humble, T. S. Quantum circuit designs of integer division optimizing T-count and T-depth. *IEEE Transactions on Emerging Topics in Computing* 9, 1045–1056 (2019).

47. Mosca, M. & Mukhopadhyay, P. A polynomial time and space heuristic algorithm for T-count. *Quantum Science and Technology* 7, 015003 (2021).

48. Ross, N. J. & Selinger, P. Optimal ancilla-free Clifford+ T approximation of z-rotations. *Quantum Inf. Comput.* 16, 901–953 (2016).

49. Jones, C. Low-overhead constructions for the fault-tolerant Toffoli gate. *Physical Review A* 87, 022328 (2013).

50. Munoz-Coreas, E. & Thapliyal, H. T-count optimized design of quantum integer

multiplication. arXiv preprint arXiv:1706.05113 (2017).

51. Gidney, C. Halving the cost of quantum addition. *Quantum* 2, 74 (2018).

52. Nam, Y., Su, Y. & Maslov, D. Approximate quantum Fourier transform with $O(n \log(n))$ T gates. *NPJ Quantum Information* 6, 1–6 (2020).

53. Selinger, P. Quantum circuits of T-depth one. *Physical Review A* 87, 042302 (2013).

54. Bocharov, A., Roetteler, M. & Svore, K. M. Efficient synthesis of universal repeat-until-success quantum circuits. *Physical review letters* 114, 080502 (2015).

55. Nielsen, M. A. & Chuang, I. L. *Quantum Computation and Quantum Information*. (Cambridge University Press, 2010).

56. Kim, T. & Choi, B.-S. Efficient decomposition methods for controlled-R_n using a single ancillary qubit. *Scientific reports* 8, 1–7 (2018).

57. Barenco, A. et al. Elementary gates for quantum computation. *Physical review A* 52, 3457 (1995).

58. Kitaev, A. Y., Shen, A., Vyalyi, M. N. & Vyalyi, M. N. *Classical and quantum computation*. (American Mathematical Soc., 2002).

59. Nam, Y. S. & Blümel, R. Scaling laws for Shor’s algorithm with a banded quantum Fourier transform. *Physical Review A* 87, 032333 (2013).

60. Nam, Y. S. & Blümel, R. Performance scaling of Shor’s algorithm with a banded quantum Fourier transform. *Physical Review A* 86, 044303 (2012).

61. Barenco, A., Ekert, A., Suominen, K.-A. & Törmä, P. Approximate quantum Fourier transform and decoherence. *Physical Review A* 54, 139 (1996).

62. Coppersmith, D. An approximate Fourier transform useful in quantum factoring. arXiv preprint quant-ph/0201067 (2002).

63. Bae, J.-H., Alsing, P. M., Ahn, D. & Miller, W. A. Quantum circuit optimization using quantum Karnaugh map. *Scientific reports* 10, 1–8 (2020).

Competing Interests

The authors declare no competing interests.

Additional Information

Supplementary Information is available in the online version of this paper. Reprints and permissions information are available online at <http://www.nature.com/reprints>.

Correspondence and requests for materials should be addressed to D.A.

Acknowledgements

This work was supported by Korea National Research Foundation (NRF) grant No. NRF-2020M3E4A1080031: Quantum circuit optimization for efficient quantum computing, NRF grant No. NRF-2020M3H3A1105796, ICT R&D program of MSIT/IITP 2021-0-01810 and AFOSR grant FA2386-21-1-0089.

Author contributions

D.A. proposed a theoretical model and wrote the main manuscript. B. P. worked out the quantum circuit decomposition, the error bound analysis, quantum computing using IonQ through Amazon Braket, and wrote the main manuscript and Supplementary Information. All authors reviewed the manuscript.